Kinetic Study on the Formation of a de Novo Designed Heterodimeric Coiled-Coil: Use of Surface Plasmon Resonance To Monitor the Association and Dissociation of Polypeptide Chains†

Heman Chao,[‡,§] Michael E. Houston, Jr.,[‡,§] Suzanne Grothe,[⊥] Cyril M. Kay,[‡,§] Maureen O'Connor-McCourt,[‡,⊥] Randall T. Irvin,[‡,∥] and Robert S. Hodges*[,‡,§]

Protein Engineering Network of Centres of Excellence, University of Alberta, Edmonton, Alberta T6G 2S2, Canada, Department of Biochemistry, University of Alberta, Edmonton, Alberta T6G 2H7, Canada, Department of Medical Microbiology and Infectious Diseases, University of Alberta, Edmonton, Alberta T6G 2H7, Canada, and Biotechnology Research Institute, the National Research Council of Canada, Montreal, Quebec, H4P 2R2, Canada

Received December 28, 1995; Revised Manuscript Received May 8, 1996[⊗]

ABSTRACT: The surface plasmon resonance (SPR) technique was used to study the formation kinetics of a *de novo* designed coiled-coil (E/K coil). The E/K coil is made up of two distinct peptides (E and K) each with five heptad (*g-a-b-c-d-e-f*) repeats. The E peptide's heptad sequence is E-V-S-A-L-E-K, and the K peptide's heptad sequence is K-V-S-A-L-K-E. A linker C-nL-G-G-G (nL = norleucine) is present at the C-terminus of the E peptide and at the N-terminus of the K peptide for the SPR studies. Heterodimer formation involves both electrostatic and hydrophobic interactions at the dimer interface. Under conditions that favor the heterodimer formation, the CD signal ($[\Theta]_{222}$) varied as a function of peptide concentration. The estimated dissociation constant (K_d) was 2.45 ± 0.71 nM. Denaturation studies with guanidine-HCl ($GdnHCl_{1/2}$ = 3.9 M) suggested a value of 3.53 ± 0.48 nM. For the SPR investigation, the peptides were biotinylated and linked to streptavidin in order to increase their effective molecular weight and consequently enhance the signal intensity. Biotinylation in itself did not impede coiled-coil formation based on CD measurements. The biosensor study revealed a slow dissociation rate constant for the heterodimer ($k_d \approx 2 \times 10^{-4}$ s^{-1}) and a moderately fast association rate constant [$k_a \approx (4.27-4.53) \times 10^5$ M^{-1} s^{-1}). This gives a calculated K_d of 0.47−0.50 nM, which agrees reasonably well with the equilibrium CD studies. Therefore, based on the SPR data, the preference for heterodimer formation is due to a combination of moderately fast association and slow dissociation rates.

The existence of an α-helical coiled-coil protein structure was first proposed by Crick (1953) based on the X-ray diffraction pattern of α-keratin. He suggested that the coiled-coil is made up of two α-helices which wrap around each other similar to a two-stranded rope. He also pointed out that nonpolar residues are more likely to be found in the interface of the two helices and the side chains of these residues would be packed in cavities formed by spaces between side chains of the opposite helix ("knobs-into-holes" packing).

One of the first supporting experimental data for this proposal came when the primary sequence of the C-terminal-half of tropomyosin was uncovered (Hodges et al., 1972; Sodek et al., 1972). The protein sequence revealed a regular heptad repeat (designated *a-b-c-d-e-f-g*) which later was shown to be transmitted throughout the entire 284-residue polypeptide chain of tropomyosin (Stone et al., 1975). The *a* and *d* positions of the heptad were occupied mostly by hydrophobic amino acids while many charged amino acids were found in the *e* and *g* locations (Hodges et al., 1972; McLachlan & Stewart 1975; Stone et al., 1975; Cohen & Parry 1990). Model building showed that the repeating hydropobes at the *a* and *d* positions could form a continuous nonpolar dimer interface (Hodges et al., 1972; Sodek et al., 1972; Stone et al., 1975) which provides the driving force for dimerization.

The importance of the hydrophobic interactions for coiled-coil stability has been studied extensively through the use of *de novo* designed synthetic peptide models [Hodges et al., 1981, 1990; Lau et al., 1984; Zhou et al., 1992a,b; Zhu et al., 1992, 1993; for reviews, please see Hodges (1992, 1996) and Adamson et al. (1993)]. It was found that the type of residues and the placement of these residues at either the *a* or *d* positions could affect the stability of the resulting coiled-coil significantly. For instance, it was observed that long chain aliphatic amino acids such as leucine at position *d* would provide much greater stability than valine or alanine in the same position. On the other hand, β-branched hydrophobes seem to be preferred at the *a* position (Hu et al., 1990; Zhu et al., 1992, 1993). This preference is due to the packing arrangement of these core amino acids caused by the distinct structural environment of the *a* and *d* positions as shown in the X-ray structure of the GCN4 leucine zipper (O'Shea et al., 1991).

† This work is supported by the Protein Engineering Network of Centres of Excellence of Canada.

* Author to whom correspondence should be addressed at Protein Engineering Network of Centres of Excellence, 713 HMRC, University of Alberta, Edmonton, AB T6G 2S2, Canada. Telephone: (403) 492-2758. Fax: (403) 492-1473. E-mail: robert.hodges@ualberta.ca.

‡ Protein Engineering Network of Centres of Excellence, University of Alberta.

§ Department of Biochemistry, University of Alberta.

∥ Department of Medical Microbiology and Infectious Diseases, University of Alberta.

⊥ National Research Council of Canada.

⊗ Abstract published in *Advance ACS Abstracts,* September 1, 1996.

S0006-2960(95)03060-1 CCC: $12.00

In addition to the core hydrophobic interactions, it is apparent that electrostatic interactions also played a significant role in coiled-coil formation and stability. Studies have shown that the interhelical ionic interactions of e−g′ and g′−e can influence the orientation of the peptide strands with respect to each other and provide for dimerization specificity (Schuermann et al., 1991; O'Shea et al., 1991 - 1993; Baxevanis & Vinson, 1993; Monera et al., 1993, 1994; Krylov et al., 1994; Zhou et al., 1994a,b; Kohn et al., 1995; Lavigne et al., 1996). Furthermore, formation of these salt bridges can reduce the solvent accessibility of the hydrophobic core, and the aliphatic side chains of the ion-paired amino acids can contribute to the core hydrophobicity, thus providing the additional stability to the coiled-coil structure (O'Shea et al., 1991).

Recently, the coiled-coil structural motif has been found in a number of DNA binding proteins (Hurst 1994). The high-resolution X-ray structures of the yeast transcription activator GCN4 leucine zipper (O'Shea et al., 1991; Ellenberger et al., 1992; König & Richmond 1993) and the heterodimeric transcription factor c-Fos-c-Jun (Glover & Harrison 1995) confirmed the "knobs-into-holes" packing arrangement of the coiled-coil. They also showed that a number of *e* and *g* charged amino acids can participate in interhelical electrostatic interactions.

Experiments with synthetic analogs of GCN4 (Harbury et al., 1993, 1994) and *de novo* designed peptides (Lovejoy et al., 1993; Betz et al., 1995; Lumb & Kim, 1995a) showed that the types of residue in the hydrophobic core could influence the oligomeric states of coiled-coils. In GCN4, it was shown that a homogeneous isoleucine interface (*a* and *d*) resulted in a trimeric coiled-coil (Harbury et al., 1994), and substitution of leucine into the *a* positions in this trimeric helix can favor tetramer formation (Harbury et al., 1993). It is apparent that, in the case of wild-type GCN4, the presence of a pair of Asn residues in the *a* position of the central heptad provides sufficient destabilization energy to disfavor the formation of oligomers while permitting the formation of a homodimer.

Although many investigations have studied the parameters that govern the stability of the coiled-coil structure, the dynamics or the kinetics of the association and dissociation processes are poorly understood. There have been only a few reports which related directly to the kinetics of coiled-coil formation or dissociation (Mo et al., 1991; Pernelle et al., 1993; Patel et al., 1994; Wendt et al., 1995; Zitzewitz et al., 1995). The knowledge of the formation kinetics is not only of theoretical interest, but it is actually of practical concern. In the case of transcription factors, the rate of formation into a functional dimer or the rate of dissociation from such a state could affect gene regulation directly. Furthermore, the coiled-coil domain has been used increasingly for novel applications. For example, the generation of miniantibodies by the fusion of a coiled-coil domain to the F_v subunits (Pack & Pluckthun 1992; Pack et al., 1995), assembly of soluble T-cell receptor (Chang et al., 1994) and IL-2 receptor (Wu et al., 1994, 1995), and the construction of chimeric proteins including transcription factors by the fusion of a coiled-coil dimerization domain to the functional domain of interest (Schmidt-Dorr et al., 1991; Taylor et al., 1991; Granger-Schnarr et al., 1992; Francis et al., 1995; Ottermann & Mekalanos, 1995; Sollerbrant et al., 1995). These few examples reveal the increased interest in using the coiled-coil domain as a dimerization motif. Therefore, the understanding of coiled-coil formation from a kinetic viewpoint becomes more important.

The goal of this investigation is two-fold. First, a *de novo* designed heterodimeric coiled-coil (E/K coil) that is suitable as a general dimerization domain is described; and second, this designed protein is used to test the applicability of the surface plasmon resonance (SPR)[1] technique (Jönsson et al., 1991; Karlsson et al., 1991) to study the coiled-coil formation kinetics. The SPR technique has been used successfully to study the kinetics of a number of bimolecular interactions including that of antigen−antibody [Green et al., 1993; Lonberg et al., 1994; please see *J. Immunol. Methods*, vol. 183 (1), for a special issue on the uses of biosensors in immunology], protein−DNA (Bondeson et al., 1993; Fisher et al., 1994), and receptor−ligand interactions (Bartley et al., 1994; Seth & Stern, 1994; Wu et al., 1995). Experimentally, it involves the immobilization of one of two interacting species to a dextran-coated gold surface and monitoring the binding of its partner presented in the solution phase. The instrument (BIAcore, Pharmacia) monitors the changes in the refractive index as a result of binding and reports the interaction in real time. The entire cycle of surface preparation, sample injection, surface regeneration, and data collection is completely automated. Thus it is possible to design and execute a large set of kinetic experiments rapidly and conveniently. To our knowledge, this is the first report that describes the use of the biosensor technology to study coiled-coil formation.

MATERIALS AND METHODS

Peptide Synthesis and Purification. The peptides were synthesized by solid-phase peptide synthesis methodology using a benzhydrylamine hydrochloride resin with conventional *N-tert*-butyloxycarbonyl (*t*-Boc) chemistry on an Applied Biosystems Model 430A peptide synthesizer (Foster City, CA) as described previously (Hodges et al., 1988). The peptides were cleaved by a mixture of hydrogen fluoride (20 mL/g resin), anisole (10%), and 1,2-ethanedithiol (2%) for 1.5 h at −5 °C. Crude peptides were extracted with glacial acetic acid and lyophilized. Freeze-dried material was dissolved in 10% acetic acid, and the solubilized peptides were purified by reversed-phase high-performance liquid chromatography (HPLC) on a Beckman System Gold HPLC system (San Ramon, California) using a Synchropak RP-4 preparative C8 column (250 × 21.1 mm i.d., 6.5 μm particle size, 300 Å pore size) (Synchrom, Lafayette, IN). A linear AB gradient of 0.2% B/min, where solvent A was 0.05% trifluoroacetic acid (TFA) in water and solvent B is 0.05% TFA in acetonitrile, and a flow rate of 5 mL/min were used to elute the peptide. Purity of the peptide was confirmed by reversed-phase analytical HPLC using a Zorbax SB 300 C8 column (250 × 4.6 mm i.d., 5 μm particle size, 300 Å pore size) (Rockland Technologies, Wilmington, DE) on a Hewlett Packard 1090 chromatography with a linear AB gradient of 2% B/min and a flow rate of 1 mL/min with solvents A and B the same as described above. The

[1] Abbreviations: TFA, trifluoroacetic acid; GdnHCl, guanidine hydrochloride; EDC, *N*-ethyl-*N*′-(3-diethylaminopropyl)carbodiimide; NHS, *N*-hydroxysuccinimide; PDEA, 2-(2-pyridinyldithio)ethaneamine; CD, circular dichroism; SPR, surface plasmon resonance; RU, resonance unit.

homogeneity and identity of the peptide were verified by amino acid analysis and mass spectrometry. For amino acid analysis, peptides were hydrolyzed in 6 N HCl at 160 °C for 1.5 h in sealed evacuated tubes. Hydrolysed material was analyzed in a Beckman Model 6300 amino acid analyzer (San Ramon, CA). Electrospray mass spectrometry was performed using a Fisons VG Quattro mass spectrometer (VG Biotech, Cheshire, England). The concentrations of the peptide solutions used in this study are obtained by amino acid analysis.

Circular Dichroism Spectroscopy. CD spectra were recorded on a Jasco J-500C spectropolarimeter (Jasco, Easton, MD) equipped with a Jasco IF500 II interface linked to an IBM PS/2 computer running the Jasco DP-500/PS2 system software (version 1.33a). The temperature of the cuvette holder is controlled by a Lauda model RMS water bath (Brinkman Instruments, Rexdale, ON). The spectropolarimeter was calibrated with an aqueous solution of recrystallized d_{10}-(+)-camphorsulfonic acid at 290.5 nm. The results are expressed as mean residue molar ellipticity [Θ] (deg cm^2 dmol^{-1}) which was calculated from

$$[\Theta] = ([\Theta]_{obs} \times MRW)/(10 \times l \times c) \qquad (1)$$

where $[\Theta]_{obs}$ is the observed ellipticity expressed in millidegrees, MRW is the mean residue molecular weight (molecular weight of the peptide divided by the number of the amino acids), l is the optical pathlength in cm, and c is the final peptide concentration in mg/mL. For wave scans, CD spectra were the average of four scans obtained by collecting data at 0.1 nm intervals from 250 to 195 nm. For urea and GdnHCl denaturation, and peptide concentration dependence studies, changes in the helical content of the samples were monitored at 222 nm and 20 °C. The buffer was 50 mM potassium phosphate, 100 mM KCl, and 10 mM DTT (pH 7.0). For the peptide concentration dependence study, a stock solution of E/K coil (100 μM) was diluted serially by a 10 mM potassium phosphate, 0.1 mM DTT buffer (pH 7.0), and the changes in helical content upon dilution were monitored at 222 nm as before. Each data point is the average of at least 24 measurements.

Sedimentation Equilibrium. Sedimentation equilibrium experiments were performed at 20 °C on a Beckman Model E analytical ultracentrifuge equipped with electronic speed control and Rayleigh interference optics. Samples were first dialyzed exhaustively against 50 mM potassium phosphate, 100 mM KCl, and 10 mM DTT (pH 7.0) at 4 °C. A 100 μL aliquot was loaded into the 12 mm double-sector, charcoal-filled Epon cell and runs (48 h) with rotor speed at 16K, 18K, 22K, and 26K rpm were performed. Samples were loaded at the initial total peptide concentrations (equimolar concentrations of the E and K peptides) of 318 μM (18K and 26K rpm), 547 μM (16K and 22K rpm), and 513 μM (22K rpm). The partial specific volumes of the peptides were calculated using the program SEQSEE (Wishart et al., 1994; Cohn & Edsall, 1943) [E = 0.73 mL/g, K = 0.76 mL/g, E/K = $(E/K)_2$ = 0.75 mL/g]. The density of the solvent was calculated to be 1.0045 g/mL. Equilibrium photographs were taken at the end of the run and fringe counts were performed on a Nikon Model 6C microcomparator. The results from all five runs were analyzed globally by the program NONLIN (Nonlinear Least Squares Analysis of Sedimentation Equilibrium Data) of Johnson et al. (1981). The program allows for the simultaneous fitting of up to 15 data sets or 8000 data points. Equilibrium data are analyzed by

$$c_{total} = \delta c + \sum_{i=1}^{n} C_i(r) = \delta c + \sum_{i=1}^{n} K_{1,i} C_1(r)^{q(i)} \qquad (2)$$

where δc is the concentration offset of the first data point, $C_i(r)$ is the concentration of the ith species at radius r, n is the total number of species present in the model being used for fitting and can be between 1 (no association) to a maximum of 5 allowed by the program, and $K_{1,i}$ and $q(i)$ are the association constant and the degree of association for the ith associated species, respectively. For fitting purposes, the term $C_1(r)$ is expanded to

$$C_1(r) = C_{1,0} \exp[\sigma(\zeta - \zeta_0) - 2B\sum_{i=1}^{n} C_i(r)] \qquad (3)$$

where $C_{1,0}$ is the monomer concentration at the first point of the data set, ζ and ζ_o are the experimental and reference $r^2/2$ values, respectively, B is the colligative second virial coefficient, and σ is the reduced molecular weight as defined by $\sigma = [M_1 (1 - \bar{\nu}\rho)\omega^2)/RT$. M_1 is the monomer molecular weight, $\bar{\nu}$ is the partial specific volume, ρ is the solvent density, and ω is the rotor speed in radians per second. The variables that can be fitted by the program are δc, ln C_{10}, qi ln $K_{1,i}$, σ, and B. Several associative models were tested. These included but were not limited to monomer ⇌ dimer, monomer ⇌ tetramer, monomer ⇌ dimer ⇌ tetramer, and dimer ⇌ tetramer equilibrium. A 95% confidence interval was set, and parameter convergence was assumed when fraction change in variance was less than 1×10^{-6} (program defaults). Since the E and K peptides were not observed to self-associate, a "pseudo" monomer with an average molecular weight of the E and K peptide was used for fitting (Lebowitz et al., 1994).

Surface Plasmon Resonance Measurements. Formation of the heterodimeric coiled-coil was monitored in real time using the BIAcore biosensor system (Pharmacia Biosensor AB, Uppsala, Sweden). The system reports changes in the refractive index near the metal surface (sensor chip) by detecting the changes in the angle of the incident light at which surface plasmon resonance occur. The principle and application of SPR detection to monitor a bimolecular interaction on the metal surface has been described in details elsewhere (Jönsson et al., 1991; Karlsson et al., 1991).

SPR-Peptide Immobilization. Coupling of the peptides (E and K) to the sensor chip CM5 was performed by the ligand thiol method (Johnsson et al., 1991). Each peptide was immobilized to produce a high (E: 170 RU and K: 455 RU) and a low (E: 51 RU and K: 63 RU) density surface for the kinetic runs. Thus, a total of four surfaces were used for the kinetic measurements. To generate the E high density surface, a continuous flow of HBS buffer (10 mM Hepes, pH 7.5, 150 mM NaCl, 3.4 mM EDTA, 0.05% Tween 20) over the sensor chip was maintained at 5 μL/min. A 10 μL injection of a solution containing 0.2 M *N*-ethyl-*N*′-(3-diethylaminopropyl)carbodiimide (EDC) and 0.05 *N*-hydroxysuccinimide (NHS) was used to activate the carboxylated dextran surface. This was followed by a 20 μL injection of 80 mM 2-(2-pyridinyldithio)ethaneamine (PDEA)

in 0.1 M borate buffer, pH 8.5. Then 25 μL of a E peptide solution (3.5 μg/mL in 50 mM formate, pH 4.0) was injected. The peptide was immobilized to the treated surface via thiol−disulfide exchange reaction. To obtain the E low density surface, only 5 μL of the EDC/NHS mixture, 10 μL of the PDEA, and 15 μL of the same peptide solution were used. The same immobilization protocol employed for the generation of the low density E surface was used to generate both K surfaces. In this case, a K peptide solution of 3.5 μg/mL (15 μL) in the formate buffer was used to generate the high density surface, and a peptide solution of 0.35 μg/mL (15 μL) was used to produce the low density surface.

SPR-Peptide Modification by Biocytin. Since the changes in refractive index as a result of coiled-coil formation on the sensor surface is relatively small due to the low molecular weight of interacting species, the peptide (either E or K) that passes over the sensor chip was modified with biocytin maleimide (biotin maleimide derivative) and streptavidin. This effectively increases the molecular weight of the dimer by a factor of 8.0, thus significantly improving the signal to noise ratio.

The protocol used for the derivatization of the peptides by biocytin maleimide was modified from that of Bayer et al. (1985). Biotin maleimide [3-(*N*-maleimidylpropionyl)-biocytin (1.1 mg); Molecular Probes, Eugene, OR] was dissolved in 400 μL of dimethylformamide and added dropwise to 3 mL of 10 mM potassium phosphate buffer (pH 7.4) containing 2 mg of either the E or K peptide with constant stirring at room temperature. This gives a reaction ratio of approximately 5 mol of biocytin maleimide to 1 mol of peptide. The modification was allowed to proceed for 3 h, and the biotin-labeled peptide was purified by reversed-phase HPLC using a Vydac C18 column (250 mm × 10 mm i.d., 5 μm particle size, and 300 Å pore size) (Supelco Canada, Mississauga, ON) with solvents and elution condition the same as described for the purification of the crude peptide. The identity and homogeneity of the modified peptide was assessed by mass spectrometry.

For all kinetics experiments, streptavidin is added to the biotin modified peptide solution at a 10-fold higher molar concentration than the biotinylated peptide. This was to ensure a preponderance of 1 mol of streptavidin to 1 mol of biotin-labeled peptide given the multivalencey of streptavidin for biotin.

SPR Measurements−Kinetic Experiments. The BIAcore instrument was programmed for iterative cycles in the kinetic experiments. Each cycle composed of (1) a 300 s peptide injection phase, (2) a 300 s dissociation phase, and (3) a 60 s regeneration phase. A flow rate of 5 μL/min was maintained throughout the cycle. HBS was used as the running and peptide buffer. An injection of 5 μL of 10 mM NaOH was used to regenerate the surface. For the E surfaces, the concentrations of biotin-K peptide used were 10, 25, 50, and 75 nM. For the K surfaces, the concentrations of biotin-E peptide used were 50, 70, 100, and 150 nM. The SPR signal was recorded in real time with sampling at every 0.5 s and plotted as RU versus time (sensorgram). Each sensorgram obtained was corrected by subtracting the initial level of SPR signal and resetting the time of injection as the origin for the purpose of data presentation and data analysis.

RESULTS

The peptides E and K are designed to form a heterodimeric coiled-coil (E/K) in neutral pH rather than the homodimers of E/E and K/K. These structural selectivity requirements are central to the usefulness of this coiled-coil as a heterodimerization domain. In order to achieve these goals, the design incorporated favorable interchain electrostatic interactions at the *e* and *g* positions for the heterodimer and selected a complementary stable hydrophobic core (*a* and *d*).

For the electrostatic feature, the heterodimer contains 10 pairs of glutamate and lysine residues with the potential to form *e* and *g* salt bridges. The methylene groups of these charged side chains could also contribute to the core hydrophobicity upon the formation of the salt bridges and further increase the overall stability as it was shown in the GCN4 structure. The favorable electrostatic interactions in the *e* and *g* positions of the heterodimer together with the unfavorable electrostatic repulsions in the similar positions of the homodimers (E/E and K/K) provide for the preference of the E/K heterodimeric conformation (Zhou et al., 1994b; Kohn et al., 1995).

The hydrophobic core of the E/K coil is constructed with the amino acids valine (*a*) and leucine (*d*). These are abundant residues found in natural coiled-coil sequences (Cohen & Parry, 1990) and synthetic peptides bearing these residues at the *a* and *d* positions seemed to favor mostly a dimeric conformation (Graddis et al., 1993; Harbury et al., 1993; Zhu et al., 1993; Kohn et al., 1995). This contrasts with an all leucine interface which could favor higher order aggregates (Harbury et al., 1993; Lovejoy et al., 1993; Lumb & Kim, 1995a). Although a leucine and valine hydrophobic core would be less stable than an all leucine one (Zhu et al., 1993), the loss in stability is partially compensated by the interchain salt bridges and, more importantly, a weaker hydrophobic core is more likely to be sensitive to modulation by the *e*−*g* interchain electrostatic interactions in the drive to form a heterodimer.

The helical wheel representation of the designed heterodimeric coiled-coil which incorporated features described above is shown in Figure 1. The E peptide has five heptad (*g-a-b-c-d-e-f*) repeats of the sequence E-V-S-A-L-E-K while the K peptide heptad sequence is K-V-S-A-L-K-E. A flexible linker, C(nL)GGG (nL = norleucine), is attached to the C-terminus of the E peptide, and a similar one is joined to the N-terminus of the K peptide. The cysteine residue of the linker provides the necessary thiol functional group for ligation to the sensor chip and serves as the acceptor for biotin for the BIAcore studies. The norleucine is included in the linker sequence to serve as an internal standard for amino acid analysis. A tyrosine residue is added to the N-terminus of the E-peptide for a purpose unrelated to this study.

The *de novo* designed E and K peptides prefer to form a heterodimeric coiled-coil (E/K) under benign conditions and at moderate concentrations. As shown in Figure 2, a solution containing 20 μM of the peptides (10 μM each of E and K) generated a CD spectrum characteristic of a fully helical conformation with minima near 208 and 222 nm. In contrast, the CD spectra of the individual peptides consisted of significant random coil structure. The ratio of $[\Theta]_{222}$ vs $[\Theta]_{208}$ of the heterodimer is 1.07, which is consistent with

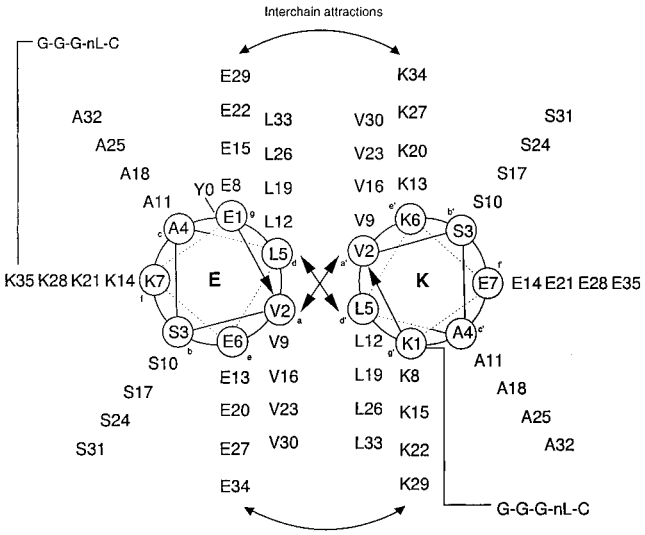

FIGURE 1: Helical wheel representation of the heterodimeric parallel E/K coil. The direction of the propagation of the polypeptide chain is into the page from the N- to the C-terminus. The E peptide is made up of five heptad (g-a-b-c-d-e-f) repeats of the sequence E-V-S-A-L-E-K and the K peptide consists of the same number of heptad repeats with the sequence K-V-S-A-L-K-E. A linker sequence, C-nL-G-G-G (nL = norleucine) is added to the C-terminus of the E peptide and the N-terminus of the K peptide. The N-terminal tyrosine (Y0) of the E-peptide is present for a purpose unrelated to this study. This diagram also depicts the a−a′, d−d′ hydrophobic interactions and the potential g−e′, g′−e interchain electrostatic interactions.

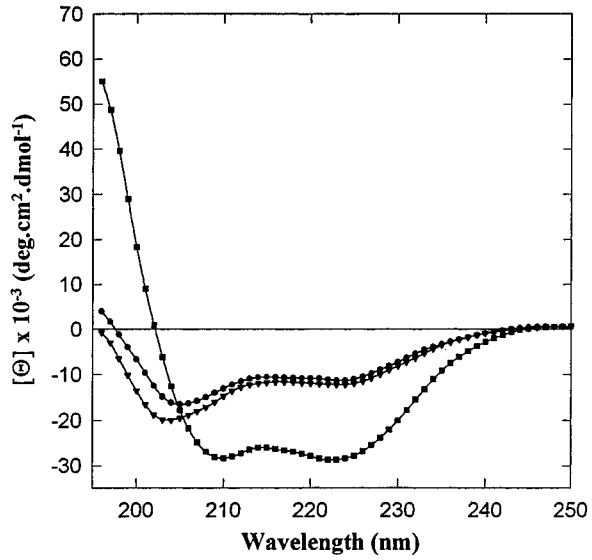

FIGURE 2: CD spectra of the heterodimeric E/K coil (■), the E (▼), and the K (●) peptide. Spectra were recorded at 20 °C in a 50 mM phosphate, 100 mM KCl, 10 mM DTT, pH 7.0 buffer. Protein concentrations were 20 μM for the E and K peptides and 10 μM each for the E and K peptides in the E/K coil sample.

previous observations that a coiled-coil structure will have a value greater than unity (Lau et al., 1984; Hodges et al., 1988; Graddis et al., 1993). Similar spectral profiles were obtained at 230 μM (1 mg/mL), a concentration at which the predominant molecular species is still a dimer as suggested by the sedimentation equilibrium study (see below).

The formation of the E/K dimer was concentration dependent. The helical content of the E/K coiled-coil varied as a function of peptide concentration. Figure 3 showed that $[\Theta]_{222}$ decreased exponentially as total peptide concentration

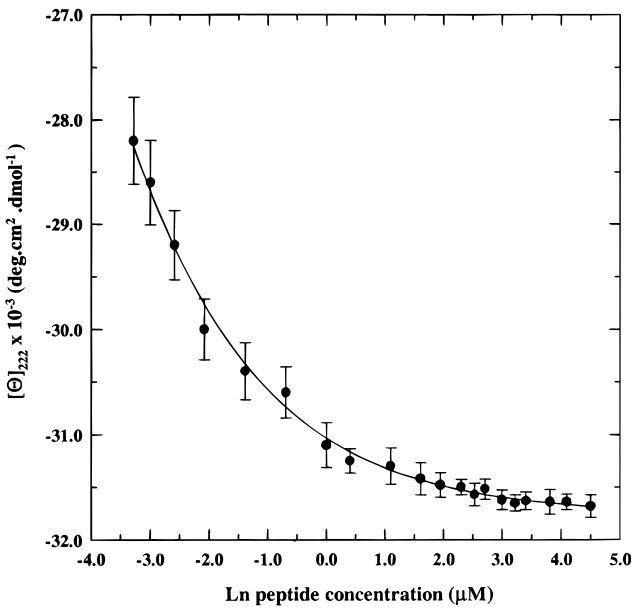

FIGURE 3: Protein concentration dependence of the mean residue molar ellipticity at 222 nm ($[\Theta]_{222}$) of the E/K coil. The $[\Theta]_{222}$ (●) was measured at 20 °C in a 10 mM phosphate, 0.1 mM DTT, pH 7.0 buffer in cells with various path lengths (0.02, 0.05, and 1.0 cm), depending on the peptide concentration. The data are fitted to a monomer ⇌ dimer model (—).

was increased from 0.0375 to 90 μM. Significant $[\Theta]_{222}$ values above baseline remained at the lowest peptide concentration (0.0375 μM) studied. Qualitatively, this suggested a small equilibrium dissociation constant (K_d). In order to estimate the value of the K_d for the dissociation of the dimer, the data (Figure 3) were fitted to a monomer−dimer model:

$$M_E + M_K = D_{E/K} \quad (4)$$

where M_E and M_K are the respective monomeric E and K peptide, and $D_{E/K}$ denotes the heterodimeric folded species. In this model, the K_d is defined as

$$K_d = [M_E][M_K]/[D]_{E/K} = 2P_t(1 - f_f)^2/f_f \quad (5)$$

where P_t is total peptide concentration, and f_f is the fraction folded. f_f is obtained from the changes in $[\Theta]_{222}$:

$$f_f = ([\Theta]_o - [\Theta]_u)/([\Theta]_f - [\Theta]_u) \quad (6)$$

where $[\Theta]_o$ is the observed molar ellipticity, $[\Theta]_u$ is the molar ellipticity for the unfolded monomer, which is taken to be −9500 deg cm^2 dmol^{-1} (Figure 2), and $[\Theta]_f$, which is the molar ellipticity of the folded coiled-coil, is a fitted parameter. Combining eqs 5 and 6 yields eq 7 for curve fitting:

$$\ln K_d = \ln [2P_t(1 - ([\Theta]_o - [\Theta]_u)/([\Theta]_f - [\Theta]_u))^2/ (([\Theta]_o - [\Theta]_u)/([\Theta]_f - [\Theta]_u))] \quad (7)$$

The K_d derived is 2.45 ± 0.71 nM (Table 1), and the $[\Theta]_f$ is −31760 ± 152 deg cm^2 dmol^{-1}.

The urea and GdnHCl denaturation profiles of the E/K coiled-coil are displayed in Figure 4. Low peptide concentration (20 μM) was used to favor the monomer ⇌ dimer equilibrium in order to obtain a free energy of unfolding for the heterodimer. Urea was not able to denature the coiled-

Table 1: Summary of Dimer to Monomer Dissociation Constants (K_d) Estimated by the Various Methods

K_d[a] ($\times 10^{-9}$ M)	$K_{d(Gdn)}$[b] ($\times 10^{-9}$ M)	$K_{d(linear)}$[c] ($\times 10^{-9}$ M)	$K_{d(nonlinear)}$[c] ($\times 10^{-9}$ M)
2.45 ± 0.71	3.53 ± 0.48	0.47 ± 0.10	0.50 ± 0.13

[a] Apparent dissociation constant and fitting error derived from nonlinear least-squares fitting the ellipticity versus protein concentration data to eq 7 (Figure 3). [b] $K_{d(Gdn)}$: dissociation constant estimated from fitting the denaturation curve to a monomer−dimer model. [c] $K_{d(linear)}$ and $K_{d(nonlinear)}$: calculated apparent dissociation constant (k_d/k_a) from the biosensor kinetic experiments based on the linear and nonlinear analyses, respectively. The k_a and k_d values are presented in Table 3. The averaged K_d from the four surfaces and the standard error are presented here.

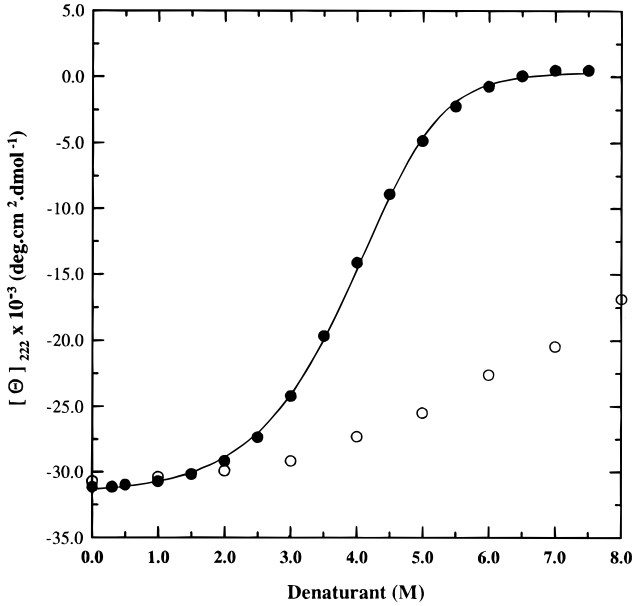

FIGURE 4: Urea (○) and GdnHCl (●) denaturation profiles of the E/K coil. The peptide concentration was 20 μM for both denaturation experiments. The GdnHCL data were fitted to a monomer ⇌ dimer model and the fitted curve (−) is also presented.

coil completely. Under these conditions, 55% of the folded ellipticity remained at 8 M urea. A combination of heat and urea was ineffective in denaturing the coiled-coil fully. Less than 15% of the starting helicity was lost at 85 °C in the presence of 5 M urea (data not shown).

In contrast, GdnHCl was able to denature the coiled-coil. A $GdnHCl_{1/2}$ of 3.9 M was observed. The ΔG_u of unfolding of the dimer was estimated by fitting the data to a monomer ⇌ dimer model described by the following equations (Milla et al., 1993; Fairman et al., 1995):

$$[\Theta]_o = f_u([\Theta]_u - \mathrm{ds}[\mathrm{GdnHCl}]) + (1 - f_u)([\Theta]_f + \mathrm{ns}[\mathrm{GdnHCl}]) \quad (8)$$

$$f_u = [-K_d + (K_d^2 + 8P_tK_d)^{1/2}]/(4P_t) \quad (9)$$

$$K_d = \exp[(-\Delta G_u + m[\mathrm{GdnHCl}]/RT)] \quad (10)$$

where f_u is fraction unfolded, ds and ns are the slopes of the denatured and native baselines, K_d the equilibrium dissociation constant, ΔG_u is the free energy of unfolding, m is the negative slope of the plot of the free energy of unfolding versus GdnHCl, $R = 1.98 \times 10^{-3}$ kcal deg mol^{-1}, and $T = 293$ K. Figure 4 showed the experimental data and the fitted

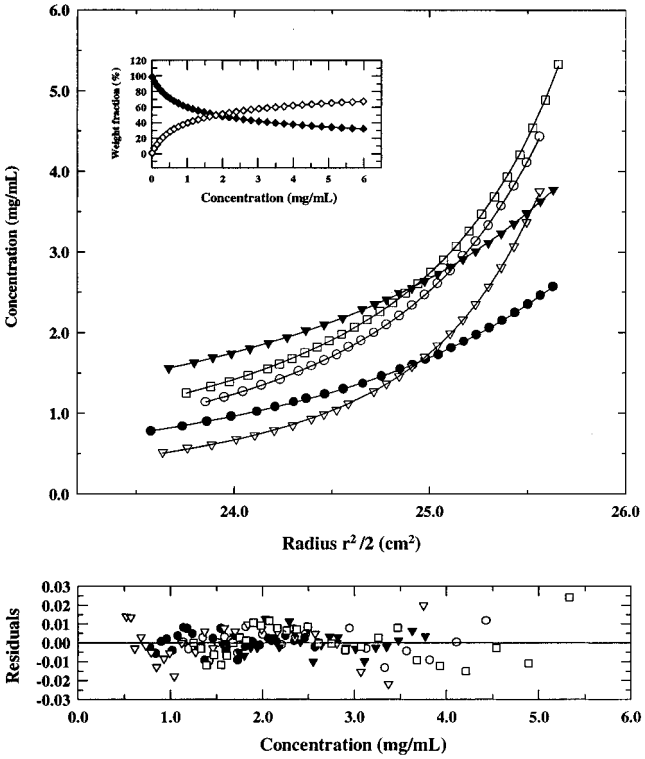

FIGURE 5: Sedimentation equilibrium studies on the E/K coil. The samples were spun in a 50 mM phosphate, 100 mM KCl, 10 mM DTT, pH 7.0 buffer for 48 h and 20 °C at various initial loading concentrations and rotor speeds (○, 513 μM and 22K rpm; ●, 318 μM and 18K rpm; ▽, 318 μM and 26K rpm; ▼, 547 μM and 16K rpm; □, 547 μM and 22K rpm. The data are fitted globally by the program NONLIN. The raw data and the fitted curves for a dimer ⇌ tetramer equilibrium are presented in the top panel. The combined residuals of the fit are presented on the bottom panel. Symbols in the residual plot correspond to data symbols from the top panel. Inset: Calculated distribution of the dimeric (◆) and tetrameric (◇) species within the concentration range observed by the sedimentation experiments (0.52−5.33 mg/mL). The amount of monomer is insignificant at these concentrations and therefore omitted from the plot for clarity. The data are calculated based on a dimer ⇌ tetramer association constant of 4.68×10^3 M^{-1} derived from the global analysis.

Table 2: Results from the Sedimentation Equilibrium Runs after Fitting to a Dimer ⇌ Tetramer Model

K_a[a] ($\times 10^3$ M^{-1})	95%[b] ($\times 10^3$ M^{-1})	fitted monomer[c] weight (Da)	95%[b] (Da)
4.68	3.62−5.78	4442	4286−4602

[a] Equilibrium association constant derived from the fitting of the sedimentation data to a dimer (E/K) tetramer $(E/K)_2$ model (RMS = 1.23×10^{-2}). [b] Respective 95% confidence intervals of the fitted parameters. [c] Monomer molecular weight predicted for the given association model. The calculated average molecular weight is 4311 Da (4227 Da for the K peptide and 4394 Da for E peptide).

curve. The ΔG_u calculated was 11.29 ± 1.61 kcal/mol, and the resulting K_d was 3.53 ± 0.48 nM (Table 1).

The sedimentation equilibrium studies showed that the E/K coil is capable of forming higher order aggregates at higher peptide concentrations (Figure 5). Global analysis of the centrifugation data indicated the present data set is best described by a dimer ⇌ tetramer model with a weak association constant of 4.68×10^3 M^{-1} (Table 2). The fitted RMS (square root of variance) was small (1.23×10^{-2}) and the distribution of the residuals was scattered (Table 2 and Figure 5). During the fitting procedure, the value of σ was

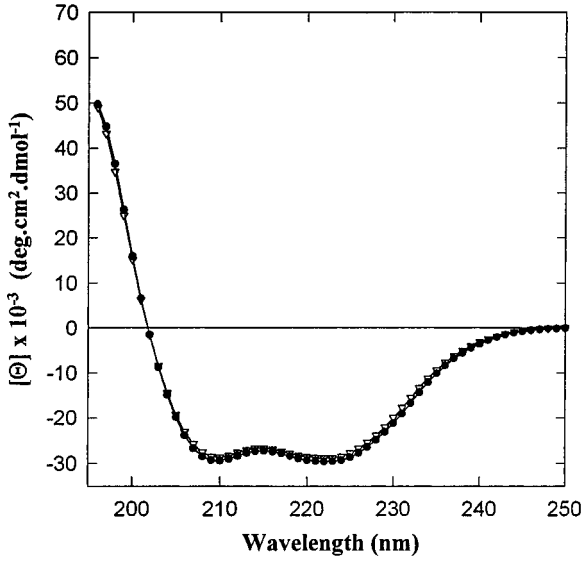

FIGURE 6: CD spectra of the heterodimeric biotinlyated E/K coil (●) and the E/biotinlyated K coil (▽). Spectra were recorded at 20 °C in a 50 mM phosphate, 100 mM KCl, 10 mM DTT, pH 7.0 buffer. Protein concentration was 20 μM for both set of samples.

first fixed at the calculated average molecular weight of the monomer, while the other variables such as ln *K* were allowed to float. Once initial approximates of the floating variables were obtained, the value of σ was also allowed to vary for the final convergence. As shown in Table 2, the fitted monomer weight agrees well with the calculated value and with reasonable symmetrical confidence interval, which indicates that the model used can describe the data adequately. A theoretical calculation showing the distribution of the dimeric and the tetrameric species within the concentration range examined (0.52−5.33 mg/mL) by the centrifugation experiments indicate that the dimeric E/K coil is preferred up to about 2 mg/mL or 0.46 mM of the monomer equivalent (Figure 5, inset).

The rate constants for the formation and dissociation of the E/K coil were estimated using the BIAcore biosensor. In order to improve the signal to noise ratio, the peptide that was in the solution phase was biotinylated and then coupled with streptavidin. Biotinylation did not impede the formation of the E/K heterodimer in solution. The CD spectra of the solutions containing equimolar concentrations of biotinylated E and K peptide, and those of E and biotinylated K peptide were virtually identical to that of the unmodified peptides (Figure 6).

The E and K peptides immobilized to the sensor surface differently. Much less of the K peptide was required to achieve a coating density similar to that of the E-peptide. This is consistent with the electrostatic requirement for peptides to be immobilized to the negatively charged dextran surface. At pH 4.0 (the immobilization condition), the K

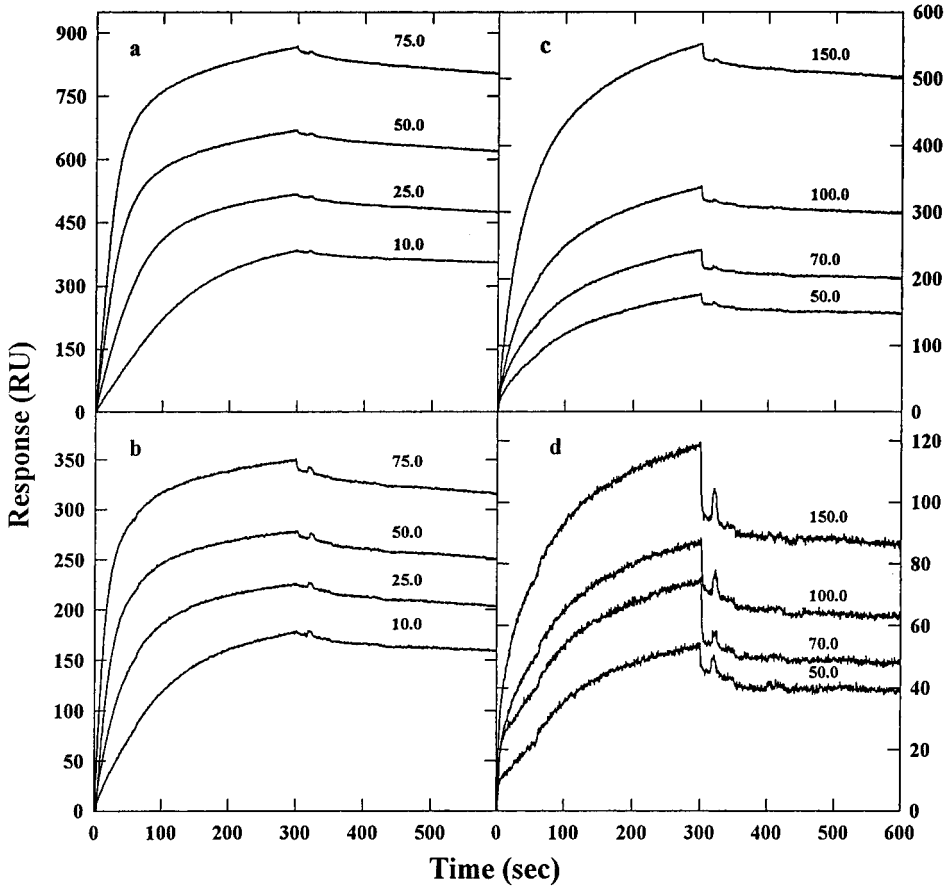

FIGURE 7: Overlaid sensorgrams showing the binding of the streptavidin/biotinylated K peptide to the (panel a) high density (170 RU) and (panel b) low density (51 RU) E surfaces and the binding of the streptavidin/biotinylated E peptide to the (panel c) high density (455 RU) and (panel d) low density (63 RU) K surfaces. Each kinetic cycle involved (1) a 300 s peptide injection phase, (2) a 300 s dissociation phase, and (3) a 60 s regeneration phase (not shown). For the E surfaces, the concentrations of the biotinylated K peptide used were 10, 25, 50, and 75 nM. For the K surfaces, the concentrations of the biotinylated E peptide used were 50, 70, 100, and 150 nM. Experiments were performed at 20 °C, and the SPR signal (RU) was recorded in real time with a sampling interval of 0.5 s. The data are presented after substraction of the baseline and repositioning the time of injection to the origin.

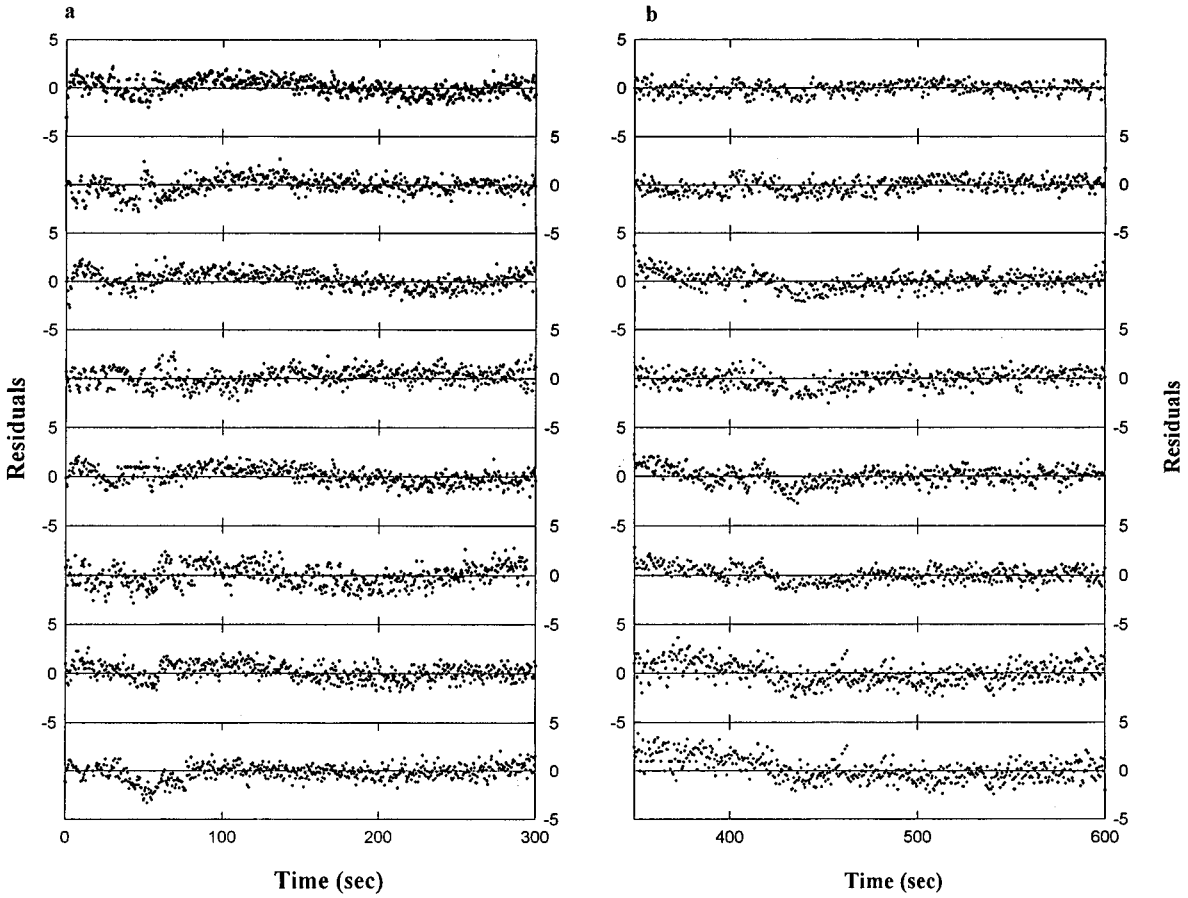

FIGURE 8: Representative residual plots from the nonlinear least-squares analysis of the association (panel a) and dissociation (panel b) phase of the SPR data. Two residual plots (the highest and lowest analyte concentrations) from each of the four sensor surfaces are shown. The order of the plots for both panels a and b starting from the top are E surface (170 RU) and 10 nM K-streptavidin, E surface (51 RU) 75 and 10 nM K-streptavidin, K surface (455 RU) 150 and 50 nM E-streptavidin, and K surface (63 RU) 150 and 50 nM E-streptavidin.

peptide has a net charge of +9.7 while the E peptide has a net charge of +3.3. However, the immobilized K peptide was less accessible than the E peptide that was coated judging from the relative maximum response that was observed under similar running conditions and analyte concentrations.

The interaction of the E and K peptides on the biosensor was specific. Control experiments (data not shown) showed that neither the biotinylated peptides nor the streptavidin alone interacted with the EDC/NHS/PDEA activated sensor surface significantly. The interaction of K-streptavidin to the corresponding E coated surface can be blocked by the presence of an excess amount of E peptide. A similar result was also observed for the E-streptavidin and K-surface interaction when an excess amount of K peptide was present. There was no evidence found for E or K peptide self-interaction at the concentration ranges used for the kinetic experiments. In fact, significant SPR signal was detected only when a mixture of E and K peptides were both present.

Figure 7 displayed the sensorgrams of the various kinetic experiments performed. The data presented have been adjusted by subtracting the baseline SPR signal at the start of the experiment and by repositioning the time of injection to the origin. The profiles of the SPR signal from all four surfaces were qualitatively similar. All of them showed a rapid SPR signal increase during the association phase of the experiment and a gradual signal reduction during the dissociation phase. None of the experiments seemed to have reached surface saturation during the 300 s injection.

The dissociation rate constant (k_d) of the E/K heterodimer was estimated by analyzing the untransformed dissociation phase of each sensorgram by nonlinear least-squares fitting to the following equation (O'Shannessy et al., 1993):

$$R = R_o \exp[-k_d(t - t_o)] \quad (11)$$

where R is the response at time t, and R_o is the initial response at start time t_o. The first 50 s of the dissociation phase was not used due to baseline instability as a result of buffer changes. Representative residual plots from each surface are shown in Figure 8b. The randomness of the residual plots and the lack of systematic deviations greater than the observed signal noise suggest that the model used was a reasonable approximation. The calculated k_d values from each sensorgram were quite similar, the values ranged from 2.06 to 2.19 $\times$ 10^{-4} s^{-1}. Table 3 summarizes the data obtained. Instead of listing 16 derived values, an average k_d for each surface is reported.

The apparent association rate constant (k_a) of coiled-coil formation on the sensor surface was determined by both the linear (Karlsson et al., 1991) and nonlinear (O'Shannessy et al., 1993) least-squares fitting procedures. The whole 300 s association phase was used for both types of analyses. For the linear analysis, the association phase of each sensorgram was first transformed to a plot of dR/dt vs R (R is the observed response unit). The resulting plot was linear which suggested that mass transport limitation was not apparent under these conditions. The k_s (the slope value) was derived

Table 3: Kinetic Constants Derived from the Surface Plasmon Resonance Studies

surface	k_a[a] ($\times 10^5$ M^{-1} s^{-1})	k_a[b] ($\times 10^5$ M^{-1} s^{-1})	k_d[c] ($\times 10^{-4}$ s^{-1})
E (170 RU)	7.41 ± 0.56	5.73 ± 1.01	2.13 ± 0.15
E (51 RU)	7.35 ± 0.71	7.58 ± 1.69	2.10 ± 0.18
K (455 RU)	1.56 ± 0.17	1.76 ± 0.20	2.19 ± 0.15
K (63 RU)	1.78 ± 0.48	1.99 ± 0.50	2.06 ± 0.16
average	4.53 ± 0.62	4.27 ± 0.82	2.12 ± 0.16

[a] Apparent association rate constant determined by linear least-squares analysis of the transformed data (Karlsson et al., 1991). The value obtained from each surface and the error of the fit are presented. [b] Apparent association rate constant determined by nonlinear least-squares analysis of the untransformed data (O'Shannessy et al., 1993). The averaged k_a value for each surface and the standard errors are shown. [c] The estimated dissociation rate constant determined by nonlinear least-squares analysis of the untransformed data (O'Shannessy et al., 1993). The averaged k_d value for each surface and the standard error are shown.

from this plot by linear least-squares analysis and was plotted against the concentration (C) of the injected peptide used on that surface (Figure 9). As shown by Karlsson et al. (1991) the k_s vs C plot is in the form of

$$k_s = k_a C + k_d \qquad (12)$$

Thus k_a can be extracted from the final plot by linear least squares fitting. The calculated k_a for each surface is presented in Table 3. Theoretically, the k_d (y intercept) can also be derived from the k_s vs C plot. However, it has been suggested that this extrapolated value is unreliable especially when the actual value of k_d is small, and it is preferable to determine the k_d from the dissociation phase of the sensorgram as it is done here for these data (Karlsson et al., 1991).

For the nonlinear analysis, untransformed sensorgrams were fitted to a model (eq 13) that describes a homogenous single-site interaction between two molecules (O'Shannessy et al., 1993):

$$R_t = R_{eq}[1 - \exp -(k_a C + k_d)(t - t_o)] \qquad (13)$$

where R is the response at time t, R_{eq} is the steady-state response level (floating variable), k_a is the association rate constant, C is the molar concentration of analyte, k_d is the dissociation rate constant as determined above, and t_o is the start time for the association. Representative residuals plots from each surface is shown in Figure 8a. Similar to the results from the dissociation phase nonlinear least-squares analyses, the profile of the residual plots suggests the model used was a reasonable approximation.

The apparent k_a values determined from the four surfaces by both type of analyses are presented in Table 3. In the case of the nonlinear least-squares analysis, an averaged k_a from the four concentrations of the injected peptides and the resulting standard error from each surface is shown. The apparent association rate constants determined were comparable among the different surfaces and between the two methods of data analyses. The calculated dissociation constants K_d (k_d/k_a) are also presented in Table 1. These data suggested that the formation of the E/K dimer was rapid, and once it was formed, it dissociated slowly to the respective monomers.

DISCUSSION

This report indicates that the SPR technique can be used successfully to study the kinetics of coiled-coil formation and dissociation. The derived parameters of k_a, k_d, and the calculated K_d, compared favorably with those obtained from equilibrium studies based on circular dichroism (Table 1) despite the fact that in the SPR studies the coiled-coil was linked to a streptavidin molecule. Although the derived rate constants were similar, there are important differences in the experimental conditions which ought to be pointed out.

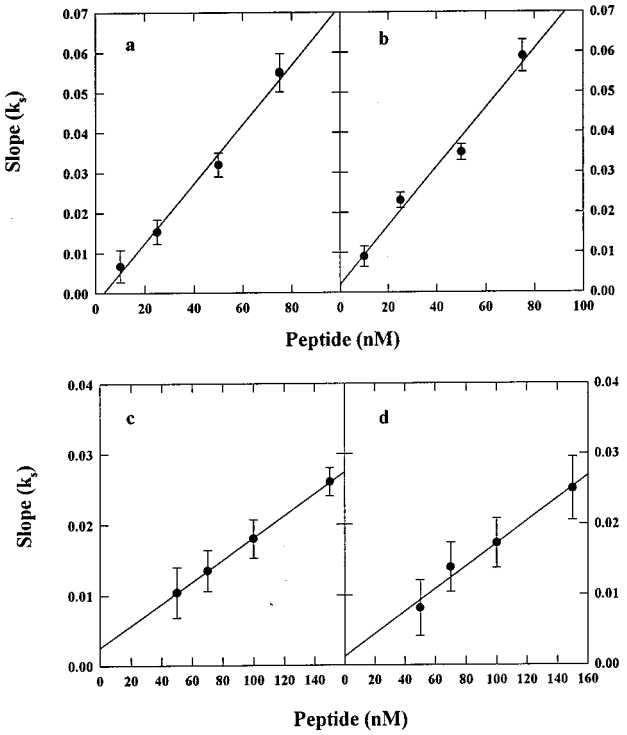

FIGURE 9: Plots of the slope values (k_s) of the dR/dt vs R plot (not shown) versus peptide concentrations for the high density (panel a) and low density (panel b) E surfaces, and the high density (panel c) and low density (panel d) K surfaces according to eq 12. The k_a (association rate constant) from each surface is extracted by linear least-squares fitting.

First, the SPR investigation is really measuring the rate of adsorption and desorption of one peptide strand to its immobilized partner. As suggested by Ward et al. (1995), this experimental condition is probably more analogous to quantitative affinity chromatography rather then solution phase bimolecular interaction. Therefore, the values of k_a or k_d obtained described a special case of bimolecular interaction where the mobility of one species is restricted.

Second, the SPR technique does not describe directly the conformational state of the coiled-coil dimer on the surface. Unlike CD studies where the observed data are directly correlated with conformation, the biosensor study is a reflection of reaction rates. Therefore, in the case of coiled-coil kinetics, the results from the biosensor studies become meaningful only if the corresponding solution state model is available. Under these assumptions, cross comparison of a set of coiled-coil forming peptides become relevant and useful.

On the basis of CD and sedimentation studies, it is clear that the *de novo* designed E and K peptides preferred the formation of a heterodimeric coiled-coil at moderate to low peptide concentrations. The dimer was very stable as it was formed at low peptide concentrations and showed resistance to urea denaturation. The corresponding small K_d reflects the stability of the dimer. From the biosensor studies, it was apparent that the stability of the dimer was manifested as a

large k_a and a small k_d. A combination of high affinity for the each other (E and K peptide) and a slow release into the monomers agreed with solution studies that the dimer was a stable entity under these conditions.

The discrepancy observed between the calculated K_d from the SPR and CD based studies can be attributed to differences in the experimental conditions, adequacy of the models to describe the observations and the accuracy of the derived parameters. On the biosensor, the predominant interaction in the environment defined is the formation of an 1:1 heterodimer. The fact that a simple A + B = AB type model seems to have accounted for the data supports this assumption. However, a second equilibrium, that is, the dissociation of the streptavidin from the biotinylated peptide, is technically possible, which could complicate the kinetic picture. In fact, there was concern initially that the attachment of a large molecule to one of the peptides might adversely affect the ability of this peptide to form a coiled-coil due to steric hindrance. The experimental observations presented here indicate that the increase in molecular weight did not reduce the affinity of the E and K peptides for each other when compared to CD studies. The streptavidin dissociation was probably inconsequential given the extremely low dissociation constant of biotin−streptavidin complex ($K_d = 10^{-15}$ M; Green, 1963) relative to the E/K coiled-coil. Furthermore, streptavidin was added to the injection buffer at a 10-fold molar excess, which should favor the biotin−streptavidin complex and, more importantly, maintain the 1:1 stoichiometry.

The small K_d observed here for the E/K dimeric coiled-coil was also seen with other coiled-coils that have very different primary sequences. For instance, studies with the Fos/Jun leucine zippers by the scintillation proximity assay (Pernelle et al., 1993) and fluorescence energy transfer method (Patel et al., 1994) suggested a dissociation constant for the heterodimer in the range of $20-100 \times 10^{-9}$ M. A thermodynamic study on the bzip protein VBP and its mutants estimated the K_d for the native homodimer to be 14×10^{-9} M (Krylov et al., 1994). A study with a *de novo* designed coiled-coil using a fluorescence technique suggested the k_{on} is in the range of 10^6 M^{-1} s^{-1} (Wendt et al., 1995). These comparisons are meant to show that the observed values for E/K coil are reasonable estimates, and no comparison is made for the folding or unfolding mechanisms of these different coiled-coils.

In summary, this study showed that the *de novo* designed E/K coil is a very stable structure. The component peptides do not self-associate in benign buffer at neutral pH and are able to form a heterodimeric coiled-coil at low peptide concentrations. The preference for the heterodimer would enable the construction of chimeric proteins with distinct functional domains. The small K_d would also ensure the predominant species in solution is the chimeric protein. These characteristics of the E/K coil indicate that the coiled-coil would be useful as a general dimerization unit.

Experiments described here also suggested that the solid-phase biosensor technology can be used to study the kinetics of coiled-coil formation. It provides an alternative kinetic picture to that of the equilibrium CD based studies. The data rationalize the stability of the dimeric coiled-coil in terms of association and dissociation rate constants. In this case, the strong preference for the heterodimer is due to a combination of slow dissociation and moderately fast association kinetics.

The example presented here is but one of the many scenarios that can be applied to the study of coiled-coils using the SPR technique. The inherent automation of the instrumentation should make experiments that involve large scale screening or systematic analysis more manageable and efficiently performed.

ACKNOWLEDGMENT

We thank Paul Semchuk, Iain Wilson, Leonard Daniels, and Lorne Burke in the peptide synthesis and mass spectrometry labs, the Alberta Peptide Institute for amino acid analysis, Bob Luty for CD spectroscopy, Leslie Hicks for sedimentation equilibrium experiments, and Dr. Pierre Lavigne for insightful discussions. This is NRC publication 39929.

REFERENCES

Adamson, J. G., Zhou, N. E., & Hodges, R. S. (1993) *Curr. Opin. Biotechnol. 4*, 428−437.

Bartley, T. D., Hunt, R. W., Welcher, A. A., Boyle, W. J., Parker, V. P., Lindberg, R. A., Lu, H. S., Colombero, A. M., Elliott, R. L., Guthrie, B. A., Holst, P. L., Skrine, J. D., Toso, R. J., Zhang, M., Fernandaz, E., Trail, G., Varnum, B., Yarden, Y., Hunter, T., & Fox, G. M. (1994) *Nature 368*, 558−560.

Bayer, E. A., Zalis, M. G., & Wilchek, M. (1985) *Anal. Biochem. 149*, 529−539.

Baxevanis, A. D., & Vinson, C. (1993) *Curr. Opin. Genet. Dev. 3*, 278−285.

Betz, S., Fairman, R., O'Neil, K., Lear, J., & DeGrado, W. (1995) *Phil. Trans. R. Soc. London B: Biol. Sci. 348*, 81−88.

Bondeson, K., Frotsell-Karlsson, Å., Fägerstam, L., & Magnusson, G. (1993) *Anal. Biochem. 214*, 245−251.

Chang, H. C., Bao, Z., Yao, Y., Tse, A. G., Goyarts, E. C., Madsen, M., Kawasaki, E., Brauer, P. P., Sacchettini, J. C., Nathenson, S. G., & Reinherz, E. L. (1994) *Proc. Natl. Acad. Sci. U.S.A. 91*, 11408−11412.

Cohen, C., & Parry, D. (1990) *Proteins 7*, 1−15.

Cohn, E. J., & Edsall, J. T. (1943) in *Proteins, Amino Acids and Peptides as Ions and Dipolar Ions*, pp 370−381, Reinhold, New York.

Crick, F. H. C. (1953) *Acta Crystallogr. 6*, 689−697.

Ellenberger, T. E., Brandle, C. J., Struhl, K., & Harrision, S. C. (1992) *Cell 71*, 1223−1237.

Fairman, R., Chao, H.-G., Mueller, L., Lavoie, T. B., Shen, L., Novotny, J., & Matsueda, G. R. (1995) *Protein Sci. 4*, 1457−1467.

Francis, M. K., Phinney, D. G., & Ryder, K. (1995) *J. Biol. Chem. 270*, 11502−11513.

Fisher, R. J., Fivash, M., Casas-Finet, J., Erickson, J. W., Kondoh, A., Bladen, S. V., Fisher, C., Watson, D. K., & Papas, T. (1994) *Protein Sci. 3*, 257−266.

Glover, J. N. M., & Harrison, S. C. (1995) *Nature 373*, 257−261.

Graddis, T. J., Myszka, D. G., & Chaiken, I. M. (1993) *Biochemistry 32*, 12664−12671.

Granger-Schnarr, M., Benusiglio, E., Schnarr, M., & Sassone-Corsi, P. (1992) *Proc. Natl. Acad. Sci. U.S.A. 89*, 4236−4239.

Green, L. C., Kortt, A. A., & Nice, E. (1993) *Eur. J. Biochem. 217*, 319−325.

Green, N. M. (1963) *Biochem. J. 89*, 585−591.

Harbury, P. B., Zhang, T., Kim, P. S., & Alber, T. (1993) *Science 262*, 1401−1407.

Harbury, P. B., Kim, P. S., & Alber T. (1994) *Nature 371*, 80−83.

Hodges, R. S. (1992) *Curr. Biol. 2*, 122−124.

Hodges, R. S. (1996) *Biochem. Cell Biol. 74*, 133−154.

Hodges, R. S., Sodek, J., Smillie, L. B., & Jurasek, L. (1972) *Cold Spring Harbor Symp. Quant. Biol. 37*, 299−310.

Hodges, R. S., Saund, A. K., Chong, P. C. S., St. Pierre, S. A., & Reid, R. E. (1981) *J. Biol. Chem. 256*, 1214−1224.

Hodges, R. S., Semchuk, P. D., Taneja, A. K., Kay, C. M., Parker, J. M. R., & Mant, C. T. (1988) *Pept. Res. 1*, 19−30.
Hodges, R. S., Zhou, N. E., Kay, C. M., & Semchuk, P. D. (1990) *Pept. Res. 3*, 123−137.
Hu, J. C., O'Shea, E. K., Kim, P. S., & Sauer, R. T. (1990) *Science 250*, 1400−1402.
Hurst, H. C. (1994) *Protein Profile 1*, 123−168.
Johnnsson, B., Löfas, S., & Lindquist, G. (1991) *Anal. Biochem. 198*, 268−277.
Johnson, M. L., Correia, J. J., Yphantis, D. A., & Halvorson, H. R. (1981) *Biophys. J. 36*, 575−588.
Jönsson, U., Fägerstam, L., Ivarsson, B., Johnsson, B., Karlsson, R., Lundh, K., Löfas, S., Persson, B., Roos, H., Rönnberg, I., Sjölander, S., Stenberg, E., Ståhlberg, R., Urabaniczky, C., Östlin, H., & Malmqvist, M. (1991) *BioTechniques 11*, 620−627.
Karlsson, R., Michaelsson, A., & Mattsson, L. (1991) *J. Immunol. Methods 145*, 229−240.
Kohn, W. D., Kay, C. M., & Hodges, R. S. (1995) *Protein Sci. 4*, 237−250.
König, P., & Richmond, T. J. (1993) *J. Mol. Biol. 233*, 139−154.
Krylov, D., Mikhailenko, I., & Vinson, C. (1994) *EMBO J. 13*, 2849−2861.
Lau, S. Y. M., Taneja, A K., & Hodges, R. S. (1984) *J. Biol. Chem. 259*, 13253−13261.
Lavigne, P., Sönnichsen, F. D., Kay, C. M., & Hodges, R. S. (1996) *Science 271*, 1136−1138.
Lebowitz, J., Kar, S., Braswell, E., McPherson, S., & Richard, D. (1994) *Protein Sci. 3*, 1374−1382.
Lonberg, N., Taylor, L. D., Harding, F. A., Trounstine, M., Higgins, K. M., Schramm, S. R., Kuo, C.-C., Mashayekh, R., Wymore, K., McCabe, J. G., Munoz-O'Regan, D., O'Donnell, S. L., Lapachet, E. S. G., Bengoechea, T., Fishwild, D. M., Carmack, C. E., Kay, R. M., & Huszar, D. (1994) *Nature 368*, 856−859.
Lovejoy, B., Choe, S., Cascio, A., McRorie, D. K., DeGrado, W. F., & Eisenberg, D. (1993) *Science 259*, 1288−1293.
Lumb, K. J., & Kim, P. S. (1995a) *Biochemistry 34*, 8642−8648.
Lumb, K. J., & Kim, P. S. (1995b) *Science 268*, 436−439.
McLachlan, A. D., & Stewart, M. (1975) *J. Mol. Biol. 98*, 293−304.
Milla, M. E., Brown, B. M., & Sauer, R. T. (1993) *Protein Sci. 2*, 2198−2205.
Mo, J., Holtzer, M., & Holtzer, A. (1991) *Proc. Nalt. Acad. Sci. U.S.A. 88*, 916−920.
Monera, O. D., Kay, C. M., & Hodges, R. S. (1993) *J. Biol. Chem. 268*, 19218−19227.
Monera, O. D., Kay, C. M., & Hodges, R. S. (1994) *Biochemistry 33*, 3862−3871.
O'Shannessy, D. J., Brigham-Burke, M., Soneson, K., Hensley, P., & Brooks, I. (1993) *Analyt. Biochem. 212*, 457−468
O'Shea, E. K., Keenan, J. D., Kim, P. S., & Alber, T. (1991) *Science 254*, 539−544.
O'Shea, E. K., Rutkowski, R., & Kim, P. S. (1992) *Cell 68*, 699−708.
O'Shea, E. K., Lumb, K. J., & Kim, P. S. (1993) *Curr. Biol. 3*, 658−667
Ottemann, K. M., & Mekalanos, J. J. (1995) *Mol. Microbiol. 15*, 719−731.
Pack, P., & Pluckthun, A. (1992) *Biochemistry 31*, 1579−1584.
Pack, P., Muller, K., Zahn, P., & Pluckthun, A. (1995) *J. Mol. Biol. 246*, 28−34.
Patel, L. R., Curran, T., & Kerppol, T. K. (1994) *Proc. Natl. Acad. Sci. U.S.A. 91*, 7360−7364.
Pernelle, C., Clerc, F. F., Dureuil, C., Bracco, L., & Tocque, B. (1993) *Biochemistry 32*, 11682−11687.
Schmidt-Dorr, T., Oertel-Buchheit, P., Pernelle, C., Bracco, L., Schnarr, M., & Granger-Schnarr, M. (1991) *Biochemistry 30*, 9657−9664.
Schuermann, M., Hunter, J. B., Henning, G., & Müller, R. (1991) *Nucleic Acids Res. 19*, 739−746.
Seth, A., & Stern, L. J. (1994) *Nature 369*, 324−327.
Sodek, J., Hodges, R. S., Smillie, L. B., & Jurasek, L. (1972) *Proc. Natl. Acad. Sci. U.S.A. 69*, 3800−3804.
Sollerbrant, K., Akusjarvi, G., Linder, S., & Svensson, C. (1995) *Nucleic Acids Res. 23*, 588−594.
Stone, D., Sodek, J., Johnson, P., & Smillie, L. B. (1975) in *Proceedings of the IX Federation of European Biochemical Societies Meeting, Protein of Contractile Systems* (Bir, E. N. A., Ed.) Vol. 31, pp 125−136, North Holland Publishing Co., Amsterdam.
Taylor, N., Flemington, E., Kolman, J. K., Baumann, R. P., Speck, S. H., & Miller, G. (1991) *J. Virol. 65*, 4033−4041.
Ward, L. D., Howlett, G. J., Hammacher, A., Weinstock, J., Yasukawa, K., Simpson, R. J., & Winsor, D. J. (1995) *Biochemistry 34*, 2901−2907.
Wendt, H., Bayer, C., Baici, A., Thomas, R. M., & Bosshard, H. R. (1995) *Biochemistry 34*, 4097−4107.
Wishart, D. S., Boyko, R. F., Willard, L., Richards, F. M., & Sykes, B. (1994) *Comp. Appl. Biosci. 10*, 121−132.
Wu, Z., Eaton, S. F., Laue, T. M., Johnson, K. W., Sana, T. R., & Ciardelli, T. L. (1994) *Protein Eng. 7*, 1137−1144.
Wu, Z., Johnson, K. W., Goldstein, B., Choi, Y., Eaton, S. F., Laue, T. M., & Ciardelli, T. L. (1995) *J. Biol. Chem. 270*, 16039−16044.
Zhou, N. E., Kay, C. M., & Hodges, R. S. (1992a) *Biochemistry 31*, 5739−5746.
Zhou, N. E., Kay, C. M., & Hodges, R. S. (1992b) *J. Biol. Chem. 267*, 2664−2670.
Zhou, N. E., Kay, C. M., & Hodges, R. S. (1994a) *Protein Eng. 7*, 1365−1372.
Zhou, N. E., Kay, C. M., & Hodges, R. S. (1994b) *J. Mol. Biol. 237*, 500−512.
Zhu, B.-Y., Zhou, N. E., Semchuk, P. D., Kay, C. M., & Hodges, R. S. (1992) *Int. J. Pept. Protein Res. 40*, 171−179.
Zhu, B.-Y., Zhou, N. E., Kay, C. M., & Hodges, R. S. (1993) *Protein Sci. 2*, 383−394.
Zitzewitz, J. A., Bilsel, O., Luo, J., Jones, B. E., & Matthews, C. R. (1995) *Biochemistry 34*, 12812−12819.

BI9530604